

# Mirror Matter, Mirror Gravity and Galactic Rotational Curves

Zurab Berezhiani<sup>1,2</sup>, Luigi Pilo<sup>1,2</sup>, and Nicola Rossi<sup>1,2</sup>

<sup>1</sup> Dipartimento di Fisica, Università di L'Aquila 67010 Coppito, AQ, Italy

<sup>2</sup> INFN, Laboratori Nazionali del Gran Sasso, 67010 Assergi, AQ, Italy

the date of receipt and acceptance should be inserted later

**Abstract.** We discuss astrophysical implications of the modified gravity model in which the two matter components, ordinary and dark, couple to separate gravitational fields that mix to each other through small mass terms. There are two spin-2 eigenstates: the massless graviton that induces universal Newtonian attraction, and the massive one that gives rise to the Yukawa-like potential which is repulsive between the ordinary and dark bodies. As a result the distances much smaller than the Yukawa radius  $r_m$  the gravitation strength between the two types of matter becomes vanishing. If  $r_m \sim 10$  kpc, a typical size of a galaxy, there are interesting implications for the nature of dark matter. In particular, one can avoid the problem of the cusp that is typical for the cold dark matter halos. Interestingly, the flat shape of the rotational curves can be explained even in the case of the collisional and dissipative dark matter (as e.g. mirror matter) that cannot give the extended halos but instead must form galactic discs similarly to the visible matter. The observed rotational curves for the large, medium-size and dwarf galaxies can be nicely reproduced. We also briefly discuss possible implications for the direct search of dark matter.

## 1 Introduction

Observational data on the Cosmic Microwave Background and on the cosmological pattern of matter distribution strongly support the presence of dark components in the Universe. The cosmological energy density being very close to the critical:  $\Omega_{tot} = \Omega_M + \Omega_A \simeq 1$ , is dominated by dark energy:  $\Omega_A \approx 0.75$ , and the rest is non-relativistic matter:  $\Omega_M \approx 0.25$ . In the latter baryons take a modest part:  $\Omega_B \approx 0.04$ , while the main fraction  $\Omega_D = \Omega_M - \Omega_B \approx 0.21$  is attributed to dark matter, a hypothetical non-baryonic component which is dark in terms of the photons but it interacts with the visible matter gravitationally.

Strong evidence for dark matter comes from the galactic rotational curves. The luminous mass is mostly concentrated in the inner core (bulge) of the galaxy. Therefore, in the absence of dark matter, the gravitational potential at large distances from the galactic center is approximately  $\phi(r) \propto 1/r$ , and the velocity of rotating matter is expected to fall as  $v(r) \propto 1/r^{1/2}$  (known as Keplerian fall-off). However, the observed rotational curves are very far from being Keplerian; in fact, in most of the disc galaxies they are nearly flat outside their bulges, i.e. velocities  $v(r)$  become approximately constant at large  $r$ .

The anomalous behavior of the rotational curves can be explained provided that dark matter forms extended, approximately spherically symmetric halos with specific density profiles [1, 2, 3]. N-body simulations show that the cold dark matter (CDM), being collisionless and non-dissipative, forms extended galactic halos, but with the density profile having a central singularity (cusp),  $\rho(r) \propto r^{-a}$ ,

where  $a$  ranges from  $a = 1$  [4], up to  $a = 1.5$  [5]. If such cusps really exist, then one can hardly reproduce the observed rotational curves [7]. For most of the galaxies, the singular profiles should manifest by a steep growth of the velocity at small distances from the center, which however does not agree with observations. Clear examples are given by the dwarf and low surface brightness (LSB) galaxies that should be dark matter dominated, but their rotational curves show no sharp rise [8]. In this respect, the non-singular profiles [2, 3] would be more satisfactory. The question whether the CDM indeed forms cusps or these are artifacts of the numerical simulations, is still debated in the literature. In particular, one might hope that the correct account for the baryon dynamics can smooth-out the singularity in dark matter profiles. But the problem potentially remains until complete and reliable computations are performed.

Many candidates have been proposed for dark matter: axion ( $m \sim 10^{-5}$  eV), sterile neutrino ( $m \sim 1$  keV), wimp ( $m \sim 1$  TeV), wimpzilla ( $m \sim 10^{14}$  GeV), etc. but its true nature is still unknown. In the context of the above candidates and popular scenarios for primordial baryogenesis there is no natural explanation for the fact that the baryon and dark matter fractions are so close,  $\Omega_D/\Omega_B \sim 5$ .

One plausible picture is that dark matter emerges from a hidden gauge sector (or sectors) which has as complex microphysics as the observable world itself. In other words, the hidden sector can have a gauge structure resembling the Standard Model of the strong, weak and electromagnetic interactions or some of its extensions. In addition, it can also have accidental conservation laws that may ren-

der some of its particles stable or very long lived, (with a lifetime bigger than the age of the Universe) exactly like the baryon number conservation in the Standard Model guarantees the proton stability.

Popular idea of *mirror world* [10,11,12] (see also [13,14]) in fact suggests that the hidden sector is just a *duplicate* of the ordinary one with exactly the same particle physics (for the reviews, see e.g. [15,16]). If the hidden mirror sector exists, then the Universe along with the ordinary particles (photon, electron, nucleons, etc.) should contain also their twins (mirror photon, mirror electron, mirror nucleons, etc.).<sup>1</sup> Turning gravity on, in the context of General Relativity (GR) the two sectors are coupled to the same metric tensor  $g_{\mu\nu}$  and the whole theory is given by the Einstein-Hilbert action

$$S = \int d^4x \sqrt{g} \left( \frac{M_{\text{P}}^2}{2} R + \mathcal{L}_1 + \mathcal{L}_2 + \mathcal{L}_{\text{mix}} \right), \quad (1)$$

where  $M_{\text{P}}$  is the reduced Planck mass and  $g = -\text{Det}[g_{\mu\nu}]$ . Here  $\mathcal{L}_1(\psi_1)$  and  $\mathcal{L}_2(\psi_2)$  are the Lagrangians respectively for the ordinary and mirror particles/fields  $\psi_1$  and  $\psi_2$ , while the ‘‘mixed’’ Lagrangian  $\mathcal{L}_{\text{mix}}(\psi_1, \psi_2)$  contains possible interaction terms as are e.g. the photon - mirror photon kinetic mixing term  $\epsilon F_1^{\mu\nu} F_{2\mu\nu}$  [17], the couplings that induce mass mixings between the ordinary and mirror neutrinos [18] and neutrons [19,20], or possible common gauge interactions between the two sectors [21]. Mirror parity, a discrete symmetry under the exchange of the two particle sets ( $\psi_1 \leftrightarrow \psi_2$ ), guarantees that the Lagrangians  $\mathcal{L}_1$  and  $\mathcal{L}_2$  are identical, i.e. ordinary (type 1) particles and mirror (type 2) particles have exactly the same characteristics (masses, coupling constants, etc.).

In spite of having the same microphysics, the two sectors cannot have the same cosmological realization. In fact, the Big Bang Nucleosynthesis bounds require that the temperature of mirror sector  $T'$  must be at least twice smaller than that of the ordinary sector  $T$  [22,23]. In addition, when  $T' < T$  mirror matter can be a viable candidate for dark matter: namely, for  $T'/T \lesssim 0.2 - 0.3$  mirror dark matter (MDM) produces the same pattern for the large scale power spectrum and the CMB anisotropies as the standard CDM [23,24,25].

In addition, if  $T' < T$  in the Early Universe, the baryon asymmetry can be generated, in both sectors, via out-of-equilibrium  $B-L$  and  $CP$  violating collision processes between ordinary and mirror particles [27] induced by those interaction terms in  $\mathcal{L}_{\text{mix}}$  that also induce the neutrino or neutron mixings with their mirror twins. Such a baryogenesis mechanism can nicely explain the puzzling ‘coin-

<sup>1</sup> In refs. [10] - [13] mirror sector was introduced for achieving formal parity restoration in weak interactions and it was identical to the ordinary one modulo its chirality: while our sector is left-handed, another sector was assumed right-handed – therefore the name *mirror* [10]. For our discussions the concerns of parity are irrelevant: parallel sector can be left-handed as well, and its particles can be called more appropriately as the *twin* electrons, the *twin* nucleons, etc. Nevertheless, in the following we shall continue to coin them as ‘mirror’.

cidence’ between the visible and dark matter fractions in the Universe, predicting the ratio  $\Omega_D/\Omega_B \sim 1 \div 10$  [16].

In contrast to the CDM, mirror baryons constitute collisional and dissipative dark matter. So one expects that the MDM should undergo a dissipative collapse and clump in galaxies instead of producing extended quasi-spherical halos.<sup>2</sup> Then, for a dark component  $M_2$  being as compact as the luminous one  $M_1$ , the gravitational potential at large distances from the galactic center would be

$$\phi(r) = -\frac{G_{\text{N}}(M_1 + M_2)}{r}, \quad G_{\text{N}} = \frac{1}{8\pi M_{\text{P}}^2}, \quad (2)$$

with  $G_{\text{N}}$  being the Newton constant. Hence, the rotational velocities should show the Keplerian fall-off  $v(r) \propto \sqrt{1/r}$  in the outer regions of the galaxies together with a steeper rise in the inner regions, both aspects contradicting the observations. Therefore, without modifying the gravity, the MDM scenario can get into serious difficulties in explaining the galactic rotational curves.

In a previous paper [28] we suggested a model for a large distance Yukawa-type modification of gravity that involves two gravitational fields. It was assumed that ordinary (type 1) matter and dark mirror (type 2) matter interact with two separate metric tensors  $g_{1\mu\nu}$  and  $g_{2\mu\nu}$ , i.e. each sector has its own GR-like gravity. The effective action of this model contains Einstein-Hilbert terms per each sector and a mixing term between the two sectors:

$$S = \int d^4x \left[ \sqrt{g_1} \left( \frac{M_{\text{P}}^2}{2} R_1 + \mathcal{L}_1 \right) + \sqrt{g_2} \left( \frac{M_{\text{P}}^2}{2} R_2 + \mathcal{L}_2 \right) + (g_1 g_2)^{1/4} (\epsilon^4 V_{\text{mix}} + \mathcal{L}_{\text{mix}}) \right], \quad (3)$$

where  $\epsilon$  is a small mass scale and  $V_{\text{mix}}(X)$  is a scalar function containing non-derivative terms built out of the two metrics through the unique available tensor combination  $X_{\nu}^{\mu} = g_2^{\mu\sigma} g_{1\sigma\nu}$ . In particular, one can have in  $V_{\text{mix}}$  terms like  $\text{Tr}(X + X^{-1})$ ,  $\text{Tr}(X^2 + X^{-2})$ , etc. (cosmological terms can be also included as  $\Lambda(\det X + \det X^{-1})$ ). As for  $\mathcal{L}_{\text{mix}}(\psi_1, \psi_2, X)$ , it again describes possible interaction terms between the ordinary and mirror particles. Now ‘mirror’ parity along with the two sets of matter fields ( $\psi_1 \leftrightarrow \psi_2$ ) exchanges also the two metric fields ( $g_{1\mu\nu} \leftrightarrow g_{2\mu\nu}$ , i.e.  $X \leftrightarrow X^{-1}$ ).

The theory admits a Lorentz-invariant vacuum solution  $\eta_{\mu\nu} = \text{diag}(-1, 1, 1, 1)$  for both metrics.<sup>3</sup> As a result, the two gravitational fields  $h_{1\mu\nu} = g_{1\mu\nu} - \eta_{\mu\nu}$  and  $h_{2\mu\nu} = g_{2\mu\nu} - \eta_{\mu\nu}$  couple to the respective energy momentum tensors  $T_{1\mu\nu}$  and  $T_{2\mu\nu}$ . The terms in  $V_{\text{mix}}(X)$  induce a mass mixing between the two gravitons. Notice that in the presence of the mixing term  $V_{\text{mix}}$  only the *diagonal* diffeomorphisms are unbroken. Hence, one eigenstate  $h_{\mu\nu} = \frac{1}{\sqrt{2}}(h_{1\mu\nu} + h_{2\mu\nu})$  (*true* graviton), that couples to both sectors symmetrically through the combination  $T_{1\mu\nu} + T_{2\mu\nu}$ , remains massless; a second eigenstate

<sup>2</sup> If the mirror matter fragmentation and mirror star formation process is fast enough, the halos can be represented by the mirror elliptical galaxies: see discussions in [23,26].

<sup>3</sup> For having a flat solution, the effective vacuum energy has to be finely tuned, as in the case of the GR.

$f_{\mu\nu} = \frac{1}{\sqrt{2}}(h_{1\mu\nu} - h_{2\mu\nu})$  which couples to the antisymmetric combination  $T_{1\mu\nu} - T_{2\mu\nu}$  gets a mass  $m_f \sim \varepsilon^2/M_{\text{P}}$ .

The theoretical consistency requires that the massive spin-2 field must have Lorentz-violating mass pattern. For this, in ref. [28] a third metric tensor  $g_{\mu\nu}^3$  was introduced that couples to both metrics in (3). So, the potential  $V_{\text{mix}}$ , apart of the combination  $X_\nu^\mu = g_2^{\mu\sigma} g_{1\sigma\nu}$ , also includes the combinations  $g_1^{\mu\sigma} g_{\sigma\nu}^3$  and  $g_2^{\mu\sigma} g_{\sigma\nu}^3$  that induce a Lorentz-violating mass terms for the eigenstate  $f_{\mu\nu}$  when the third metric gets the Lorentz-breaking vacuum configuration  $\eta_{\mu\nu}^3 = \text{diag}(-c^2, 1, 1, 1)$  [29]. (Technically, the third metric can be rendered non dynamical in a suitable limit, and the dynamical effects of the ‘third’ graviton can be neglected). The same goal can be achieved by a dynamical Lorentz-breaking condensate [30]. The models of massive gravity (bigravity) with the Lorentz invariance [31,32] have serious theoretical problems while giving up the Lorentz invariance allows to have a healthy ghost-free theory.<sup>4</sup> In addition, such a theory does not suffer from the Van Dam-Veltman-Zakharov discontinuity problem [28,29,34]. Regarding the experiments for the light deflection and light travel time our model has no deviation from the GR predictions (i.e. in terms of the Post-Newtonian parameters  $\gamma_{\text{PPN}} = 1$ ). The exact spherically symmetric solutions for a Lorentz-breaking massive bigravity were found in ref. [35]. The parametrized Post-Newtonian limit of the bigravity theories were recently studied in ref. [36].

Theoretical aspects of the model are discussed in details in [28,37]. For what concerns us, the bottom line is that it leads to interesting long-distance modification of the gravity. Namely, taking a point-like source composed of both type 1 and type 2 masses,  $M_1$  and  $M_2$ , the exchange of massless graviton  $h_{\mu\nu}$  induces the following potential for the both type 1 and type 2 test particles:

$$\phi_h(r) = -\frac{G_h(M_1 + M_2)}{r}, \quad G_h = \frac{1}{16\pi M_{\text{P}}^2} \quad (4)$$

On the other hand, the massive graviton  $f_{\mu\nu}$  coupled to the anti-symmetric combination of  $M_1$  and  $M_2$  induces the following Yukawa-like potential for a type 1 test particle:

$$\phi_f(r) = -\frac{G_f(M_1 - M_2)e^{-\frac{r}{r_m}}}{r}, \quad G_f = \frac{1}{16\pi M_{\text{P}}^2} \quad (5)$$

while for a type 2 test particle the potential is  $-\phi_f(r)$ . The Yukawa radius is defined by the Compton wavelength of the massive graviton,  $r_m = 1/m_f$ . This potential is *repulsive* between the type 1 and type 2 matter. As far as  $G_f = G_h = G_{\text{N}}/2$ , the universal attraction (4) between the latter is exactly cancelled by this repulsion in the limit  $r/r_m \rightarrow 0$ . Hence, at small distances,  $r \ll r_m$ , there is practically no gravitation between the ordinary matter and dark matter objects.<sup>5</sup>

<sup>4</sup> Under certain assumptions, one can prove a theorem [33] that there cannot exist consistent (ghost-free) interactions of two massless gravitons. This proof, however, does not apply to our model [28] where the spin-2 field  $f_{\mu\nu}$  is massive and moreover its mass terms are Lorentz non-invariant.

<sup>5</sup> Let us remark that the equality  $G_f = G_h$  is not generic: e.g., for  $f_{\mu\nu}$  with the Lorentz-invariant (Fierz-Pauli) mass term

The full potential felt by an ordinary test particle  $\phi(r) = \phi_h(r) + \phi_f(r)$  can be presented as:

$$\phi(r) = -\frac{G_{\text{N}}(1 + e^{-\frac{r}{r_m}})M_1}{2r} - \frac{G_{\text{N}}(1 - e^{-\frac{r}{r_m}})M_2}{2r}, \quad (6)$$

while the corresponding potential for a type 2 test particle,  $\phi_-(r) = \phi_h(r) - \phi_f(r)$ , is obtained from (6) by exchange  $M_1 \leftrightarrow M_2$ . Hence, at small distances the universal character of gravity between the ordinary and dark components is violated. This is acceptable as far as there are no experimental data regarding the gravitational interactions of dark matter at small distances. On the other hand, at  $r \ll r_m$  gravity between type 1 bodies (as well as between type 2 bodies) remains essentially standard: one has the Newton law with a constant  $G_{\text{N}}$  and the weak equivalence principle is respected for all kinds of visible matter. These properties are verified with a spectacular precision in a wide range of distances: from a fraction of mm (terrestrial experiments) to several AU (solar system tests). Therefore, our potential (5) does not conflict with the experimental data provided that the Yukawa radius is much larger than the solar system, say  $r_m \gg 20 \text{ AU} = 10^{-4} \text{ pc}$ .

At large distances,  $r \gg r_m$ , the massive spin-2 field decouples: the Yukawa term  $\phi_f(r)$  (5) dies out and only the long-range potential  $\phi_h(r)$  (4) remains at work, which is universal between type 1 and type 2 components. Obviously, the latter is just the same as the familiar Newtonian potential (2) but with a *halved* Newton constant  $G_h = G_{\text{N}}/2$ . Variation of the Newtonian constant with the distance, however, would not contradict the observational data if the Yukawa radius is larger than few pc, the distance scale at which the systems of the gravitationally bounded stars still can be tested.

Interesting features can emerge at intermediate distances  $r \sim r_m$  where both potentials (4) and (5) are important. In particular, in this paper we take  $r_m \sim 10 \text{ kpc}$ , a typical optical size of galaxies. This will allow us to explain the nearly flat shape of the galactic rotation curves even if dark matter does not form extended halos but it collapses into discs similarly to the visible component, exactly what is expected in the case of mirror matter.

The paper is organized as follows. In the next section we discuss the case of point-like type 1 and type 2 sources and the corresponding modification of the Newton law at large distances. In section 3 we study the implications for the galactic rotational curves. Finally, in section 4, we shortly discuss our results and outline the implications of our scenario for the direct search of dark matter.

one would have  $G_f = \frac{4}{3}G_h$  and a sick theory suffering from the discontinuity problem and other diseases. In our model  $G_f = G_h$  is due to the Lorentz-breaking in the mass terms for  $f_{\mu\nu}$ . In general case the Lorentz-breaking originates *two* Yukawa terms of the type (5) with the different radii  $r_{1m}$  and  $r_{2m}$  [28]. In this paper, for the sake of simplicity, we take them equal,  $r_{1m} = r_{2m} = r_m$ .

## 2 Modified Newton Law

In this section we show that at distances  $r \sim r_m$ , the typical rotational velocities of an ordinary test body in the gravitational field produced by mirror matter has a rather flat shape even if the source is point-like.

The free fall acceleration of a type 1 test particle in the potential (6) reads:<sup>6</sup>

$$\begin{aligned} g(r) &= \frac{G_N}{2} \left[ \frac{M_1 + M_2}{r^2} + \frac{M_1 - M_2}{r^2} \left( 1 + \frac{r}{r_m} \right) e^{-\frac{r}{r_m}} \right] \\ &= \frac{G_+(r)M_1}{r^2} + \frac{G_-(r)M_2}{r^2} \end{aligned} \quad (7)$$

where the effective ‘‘Newton’’ constants  $G_{\pm}$  become distance dependent functions:

$$\frac{G_{\pm}(r)}{G_N} = \frac{1}{2} \left[ 1 \pm \left( 1 + \frac{r}{r_m} \right) e^{-\frac{r}{r_m}} \right], \quad (8)$$

so that  $G_+(r) + G_-(r) = G_N$  (see Fig. 1). Namely,  $G_+(r)$  measures the gravitational strength between the two type 1 objects (and between two type 2 objects) while  $G_-(r)$  the strength between the type 1 and type 2 objects.

At small distances,  $r \ll r_m$ , we have:

$$\frac{G_+(r)}{G_N} \approx 1 - \frac{1}{4} \left( \frac{r}{r_m} \right)^2, \quad \frac{G_-(r)}{G_N} \approx \frac{1}{4} \left( \frac{r}{r_m} \right)^2. \quad (9)$$

In the limit  $r \rightarrow 0$  we get  $G_+ = G_N$  while  $G_-$  vanishes. Thus, at small distances the gravitational force between ordinary objects obeys the universal  $1/r^2$  Newton law with a constant  $G_N$ , while dark matter becomes dark also for the gravity. More precisely, at  $r \ll r_m$  the acceleration of a test particle in the field of dark point-like source  $M_2$  is constant but very small,  $g_-(r) = G_N M_2 / 4r_m^2$ .

At large distances,  $r \gg r_m$ , we get

$$\frac{G_+(r)}{G_N} = \frac{G_-(r)}{G_N} = \frac{1}{2} \quad (10)$$

with the precision of exponentially small terms. Thus, in the limit  $r \rightarrow \infty$ , the gravitational force between ordinary and dark matter becomes universal and  $\propto 1/r^2$  but with a *halved* Newton constant  $G_N/2$ .

For  $r_m \sim 10$  kpc, the gravity modification effects are too small and have no impact for the solar system tests: eq. (9) shows that the sun and its planets gravitate with the same Newton constant  $G_N$  that is experimentally measured in small distance experiments on the Earth, up to correction less than  $(20 \text{ AU}/10 \text{ kpc})^2 \sim 10^{-16}$ . On the other hand, dark (mirror) objects have almost no attraction to the sun and within the solar system their acceleration is practically vanishing:  $g_2 = G_N M_{\odot} / 4r_m^2 \approx 4 \times 10^{-20} \text{ cm/s}^2$ .

<sup>6</sup> Observe that for  $M_1 = M_2$  the Yukawa term becomes ineffective and the acceleration is exactly the same as the one induced by the source  $M_1$  in the case of normal Newtonian gravity:  $g(r) = G_N M_1 / r^2$ .

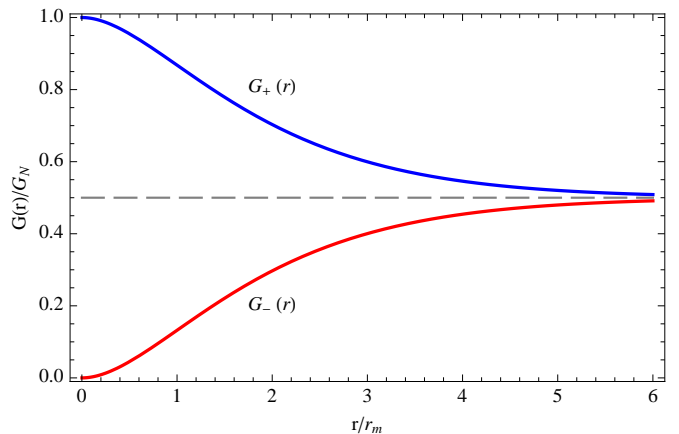


**Fig. 1.** The distance dependent ‘‘constants’’  $G_+(r)$  (upper curve) and  $G_-(r)$  (lower curve), in units of the experimental Newton constant  $G_N$ .

On the other hand, at large distances the exponential term in (8) dies out and e.g. for  $r > 1$  Mpc, within a precision better than  $10^{-41}$  we recover the universal  $1/r^2$  force law but with the *halved* Newton constants  $G_{\pm} = G_N/2$ . Thus, as far as the present cosmological expansion and formation of the large scale structures are concerned for which the horizon crossing scales are much larger than  $r_m \sim 10$  kpc, all should remain nearly as in the standard FRW cosmology with the Newton constant being  $G_N$  at all distances. However, for a given value of the Hubble constant, the total energy density of the Universe in the context of our model should be  $\rho_{\text{our}} = 3H_0^2/4\pi G_N$  instead of  $\rho \approx \rho_{\text{cr}} = 3H_0^2/8\pi G_N$ . Hence,  $\rho_{\text{our}} \approx 2\rho_{\text{cr}}$  [28]. Moreover, once in our scenario the large scale structures with comoving scales larger than few Mpc are governed by a *halved* Newton constant,  $G_N/2$ , it is natural to expect that the proportion between the dark matter and baryon densities in the Universe is also a factor of 2 larger than the ratio  $\rho_D/\rho_B \simeq 5$  required in the standard cosmological ‘concordance’ model. In other words, in order to keep the gravitational dynamics of large structures like galaxy clusters and superclusters compatible with the observations, one must take  $\beta_{\text{cosm}} = \rho_2/\rho_1 \simeq 10$ . As in the standard cosmology, in our scenario the dominant contribution in total energy density of the Universe should come from some sort of dark energy.

However, at intermediate distances the Yukawa-like term is essential: for  $r \sim r_m$  the constants  $G_+$  and  $G_-$  are comparable but not equal. For  $r_m \sim 10$  kpc, this can have interesting consequences for the testing the dark matter in the galaxies.

In order to grasp the basic idea behind the shape of the rotational curves produced by the potential (6), let us imagine a galactic object moving along a circular orbit of radius  $r$  from the center. Its velocity is determined by equating the centrifugal force with the radial component of gravitational pull, i.e.  $v^2(r)/r = g(r)$ . Therefore, in the Newtonian case,  $g(r) = G_N M / r^2$  the rotational velocity is Keplerian:  $v(r) = (G_N M / r)^{1/2}$ ;  $M = M_1 + M_2$  represents the total mass of the source, regardless is dark or visible.

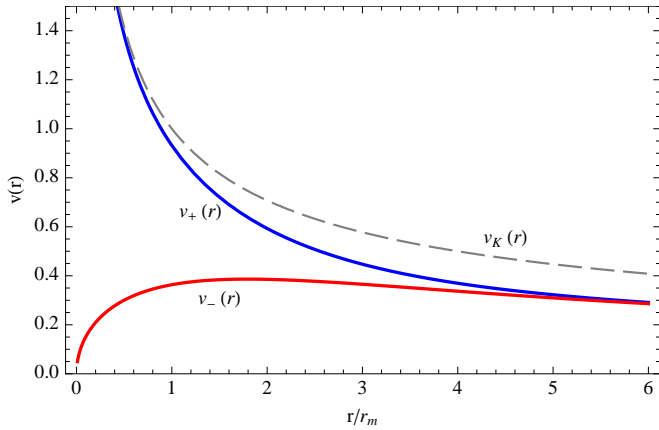


**Fig. 2.** Rotational velocities in our model (arbitrary units) for a point-like ordinary (type 1) source with a given mass  $M_1 = M$  ( $v_+$ , upper solid) and for a mirror (type 2) source with  $M_2 = M$  ( $v_-$ , lower solid). For a composite source with  $M_1 = M_2 = M$ , the rotational curve exactly coincides with the Keplerian one,  $v_K(r) = \sqrt{G_N M/r}$ , originated by the mass  $M$  in the standard Newtonian gravity (dash).

In our case, the acceleration (7) has to be used and the situation is different. For an ordinary source  $M_1$  we have  $v_+(r) = [G_+(r)M_1/r]^{1/2}$ , and the velocity fall-off at distances  $r \sim r_m$  is even faster than in the Keplerian case (see upper solid curve in Fig. 2). However, the rotational velocity in the field of a mirror source  $M_2$ ,  $v_-(r) = [G_-(r)M_2/r]^{1/2}$ , has a quite different shape. At small distances it increases (approximately as  $r^{1/2}$ ) approaching a rather smooth plateau around  $r \sim r_m$  and then decreases very slowly (see lower curve in Fig. 2).

This gives a hint that in our modified gravity model one can reproduce the observed rotational curves if  $r_m \sim 10$  kpc even without requiring that dark matter forms extended halos. Instead, it can be distributed in the galaxy in a rather compact way as it is natural for mirror matter. Fig. 2 shows that a typical rotational curve produced by a dark source is rather flat within a wide range of distances,  $r/r_m \sim 1 \div 5$ , even if the source is point-like. (Obviously, the curves should flatten more when the dark source is extended with a radius comparable to  $r_m$ .) In addition, Fig. 2 gives also an idea that the dark matter cusp, if it exists, can become harmless for the observations: it will be gravitationally ‘invisible’ for the stars rotating closer to the galaxy center and the rotational curves at small distances will not be affected. Needless to say, for achieving the correct rotational profiles the amount of dark matter  $M_2$  in the galaxy should be considerably bigger than that of visible matter  $M_1$ .

### 3 Galaxy Rotational Curves

Rotational curves describe the velocity  $v(r)$  of gravitationally bounded galactic objects (typically stars and interstellar gas) as a function of the distance  $r$  from the center. The square of the rotational velocity  $v^2$  has then two contributions: one from the visible matter and another from

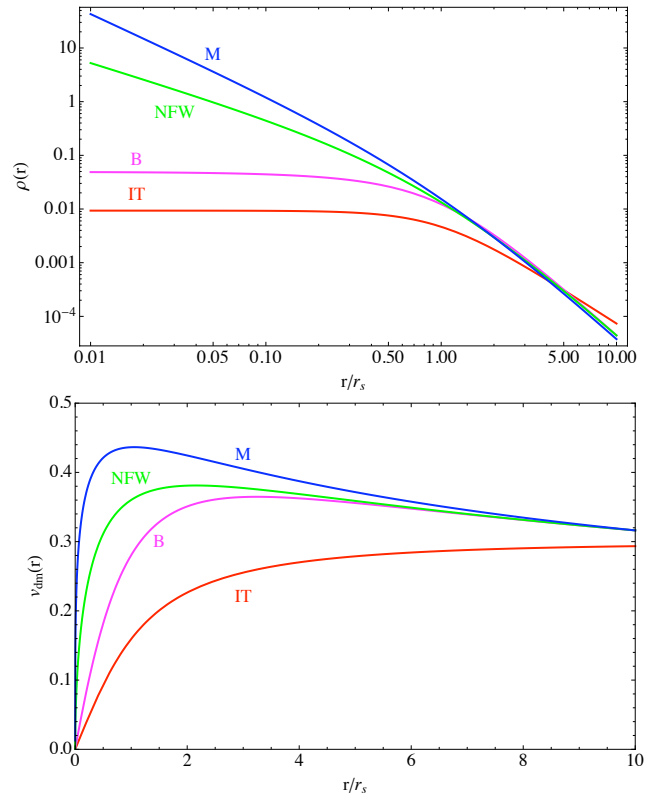


**Fig. 3.** Density profiles  $\rho(r)$  for the IT, Burkert (B), NFW and Moore (M) models and the respective curves for  $v_{\text{dm}}(r)$ .

the dark matter:

$$v^2(r) = v_{\text{vis}}^2(r) + v_{\text{dm}}^2(r). \quad (11)$$

The form of  $v_{\text{vis}}^2$  depends on the distribution of matter in the galaxy. In ‘honest’ disk galaxies visible matter is distributed along the disk with the profile (minimum disc hypothesis[38]):

$$\sigma_1(r) = \frac{M_1}{2\pi r_1^2} e^{-r/r_1}. \quad (12)$$

The central density is normalized by the total visible mass  $M_1$  and  $r_1$  is the length scale of the disc. Thus, in the absence of dark matter, the rotational velocities for  $r \gtrsim 2r_1$  are expected to fall off according to Keplerian behavior  $v(r) \propto \sqrt{1/r}$ . One observes instead that in the outer regions of galaxies the rotational curves flatten, i.e.  $v(r)$  is approximately constant. More precisely, for all spiral galaxies the rotational curves are not really flat but still far from the expected Keplerian fall-off. Empirically, the observational data of many galaxies are well fitted by the so called universal rotational curves [9].

The dark matter distribution in galaxies depends on its nature but also on various subtle details of the galaxy formation. Several models are considered in the literature. For example, the pseudo-isothermal (IT) profile [2] is obtained by taking an isothermal equation of state for matter in hydrostatic equilibrium in the presence of Newtonian

gravity with a suitable boundary conditions. It has a form

$$\rho(r) = \frac{\rho_s}{1 + \frac{r^2}{r_s^2}}, \quad (13)$$

where  $\rho_s$  is the central density and  $r_s$  is a characteristic length scale defining the size of the constant density core. At large distances,  $r \gg r_s$ , the density drops as  $r^{-2}$ . Therefore, at  $r \gg r_s$  the mass  $M(r) = \int_0^r 4\pi r'^2 \rho(r') dr'$  grows linearly with  $r$ , and hence the rotational velocity  $v_{\text{dm}}(r) = \sqrt{G_N M(r)/r}$  becomes constant at large distances. For realistic cases, the divergence of  $M(r)$  should be cut-off at some proper distance from the galaxy center.

Another core-like profile was suggested by Burkert [3]:

$$\rho(r) = \frac{\rho_s}{\left(1 + \frac{r}{r_s}\right)\left(1 + \frac{r^2}{r_s^2}\right)}. \quad (14)$$

In this case, for large  $r$  the density falls as  $\rho \propto r^{-3}$ , and thus  $v_{\text{dm}} \propto (\ln r/r)^{1/2}$ .

Numerical N-body simulations for the CDM produce the following density profiles:

$$\rho(r) = \frac{\rho_s}{\left(\frac{r}{r_s}\right)^a \left[1 + \left(\frac{r}{r_s}\right)^a\right]^{\frac{3}{a}-1}}, \quad (15)$$

which have a singularity (cusp) for small  $r$ :  $\rho \sim r^{-a}$ , with the value  $a$  depending on the simulation details. In particular,  $a = 1$  for the Navarro-Frenk-White (NFW) model [4] and  $a = 1.5$  for the case of Moore et al. [5]. For large  $r$  one has  $\rho \propto r^{-3}$  in both cases. Different density profiles for dark matter and their contributions  $v_{\text{dm}}(r)$  to the rotational velocities are schematically shown in Fig. 3.

From the empirical side, the non-singular IT or B profiles can nicely fit most of the observed rotational curves, even those for the dark matter dominated galaxies as are the dwarf and LSB galaxies [2, 3]. However, from the theoretical side, these core-like profiles are not favored by the numerical computations in the CDM picture which point instead towards the singular profiles (15) that predict too steep rise of the rotational velocity at small distances which feature should be more prominent in the case of the galaxies dominated by dark matter. This however is in contradiction with the shallow shapes of the rotational curves observed for the dwarf and LSB galaxies [6].

The following remark is in order. The fits show that, with the exception of the low-luminosity dwarfs, the visible component makes the dominant contribution to the rotational velocities within the bright optical disc [2]. The appearance of flat rotational curves does in general require a careful matching of the falling contribution  $v_{\text{vis}}(r)$  from the disc and the rising contribution  $v_{\text{dm}}(r)$  from the halo – the ‘‘conspiracy’’. In the dwarf and LSB systems this conspiracy generally breaks down as far as the halo contribution  $v_{\text{dm}}(r)$  becomes dominant already within the optical disc.

Let us now discuss how the rotational curves can be obtained using the modified gravitational potential (6), without assuming extended dark halos. The key proposal

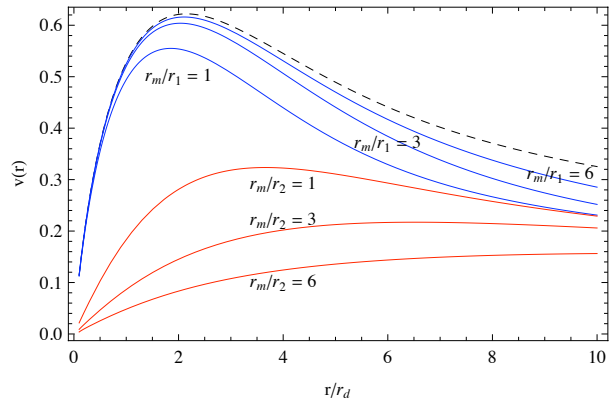


**Fig. 4.** Contributions to rotational velocities in our model (arbitrary units). The dash curve shows the rotational velocity in the visible matter disc with a radius  $r_d = r_1$  in the case of normal Newtonian gravity. The three upper solid curves correspond to  $v_{\text{vis}}$  for the same ordinary disc in our model for different values of  $r_m$ , and the three lower solid curves correspond to  $v_{\text{dm}}$  for the mirror matter disc with  $r_d = r_2$ .

is to use dark matter the *similar* density profiles for luminous and dark matter. Hence, the two components are assumed to be distributed in two overlapping concentric disks with similar density profiles. Namely, we take exponential distribution (12) for visible matter and assume the analogous form for dark matter obtained by rescaling  $M_1 \rightarrow M_2$  and  $r_1 \rightarrow r_2$ :

$$\sigma_1(r) = \frac{M_1}{2\pi r_1^2} e^{-\frac{r}{r_1}}, \quad \sigma_2(r) = \frac{M_2}{2\pi r_2^2} e^{-\frac{r}{r_2}}, \quad (16)$$

where  $M_2$  is a total dark mass in the galaxy and  $r_2$  is length scale of its distribution. For mirror dark matter this hypothesis is quite natural: it has the same microphysics as ordinary (baryonic) matter; it is then conceivable that the very same mechanism of galaxy formation operates in both sectors giving the same matter distributions up to a rescaling of the relevant parameters.

The acceleration of a test type 1 particle located at the coordinates  $\mathbf{r} = (x, y)$  on the disc can be readily found:

$$\mathbf{g}(\mathbf{r}) = \frac{G_N}{2} \int_{\text{Disk}} r' dr' d\vartheta \frac{(\mathbf{r} - \mathbf{r}')}{|\mathbf{r} - \mathbf{r}'|^3} \left[ \sigma_1(\mathbf{r}') + \sigma_2(\mathbf{r}') \right] + [\sigma_1(\mathbf{r}') - \sigma_2(\mathbf{r}')] \left( 1 + \frac{|\mathbf{r} - \mathbf{r}'|}{r_m} \right) e^{-\frac{|\mathbf{r} - \mathbf{r}'|}{r_m}}, \quad (17)$$

where  $|\mathbf{r} - \mathbf{r}'| = \sqrt{r^2 + r'^2 - 2rr' \cos \vartheta}$ . Due to cylindrical symmetry,  $v(r) = \sqrt{rg(r)}$  will depend only on the radius  $r = (x^2 + y^2)^{1/2}$ . For the exponential density distributions (16) the integration can be performed semi-analytically.

In Fig. 4 we show typical shapes for the ordinary and dark contributions,  $v_{\text{vis}}(r)$  and  $v_{\text{dm}}(r)$ , for different ratios between the Yukawa radius  $r_m$  and the disc lengths  $r_d = r_1, r_2$ . Notice the apparent similarities between the (lower) curves for  $v_{\text{dm}}(r)$  in Fig. 4 and the ones in Fig. 3 obtained for the IT and Burkert halos in the case of the normal gravity.

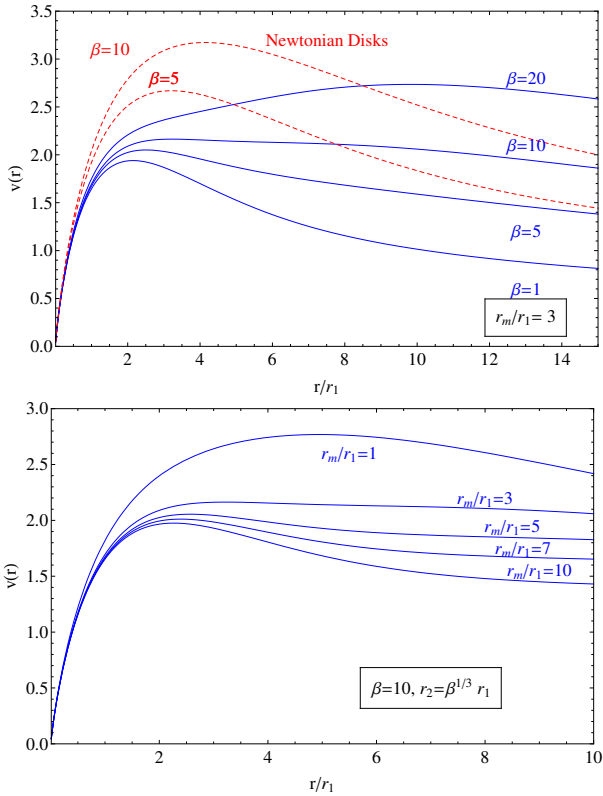


**Fig. 5.** Rotational curves for different values of  $\beta = M_2/M_1$  with  $\nu = r_m/r_1$  fixed (upper panel) and for different values of  $\nu$  with  $\beta$  fixed (lower panel). The dotted curves refer to the velocity curves originated by the superimposed dark and visible discs in the case of unmodified Newtonian potential.

It is convenient to introduce the rescaling factors between the characteristics of the ordinary and dark discs:

$$r_2 = \alpha r_1, \quad M_2 = \beta M_1. \quad (18)$$

The parameters  $\alpha$  and  $\beta$  can differ from galaxy to galaxy, while the gravitational radius  $r_m$  must be the same for all galaxies. In fact, the values of  $\alpha$  and  $\beta$  determine the weights by which the curves for  $v_{\text{vis}}(r)$  and  $v_{\text{dm}}(r)$  shown on Fig. 4 for different  $r_m/r_{1,2}$  should be superimposed quadratically for obtaining the rotational velocity  $v^2(r)$  (11). Hence, the shape of the rotational curve produced by the modified gravitational potential (6) for a given galaxy should be controlled by the three ratios  $\beta = M_2/M_1$ ,  $\alpha = r_2/r_1$  and  $\nu = r_m/r_1$ .

Rotational curves predicted for different choices of the relevant parameters are presented in Figs. 5. In particular, the upper panel of Fig. 5 shows how the shapes of rotational curves depend on  $\beta$  for a fixed  $\nu = 3$ , i.e. when the graviton radius  $r_m$  is taken equal to three times the disc length scale, which is about the optical radius of the galaxy. For  $r_m \sim 10$  kpc, this would correspond to the case of the reasonably large galaxies like the Milky Way. On the other hand, for large galaxies the ratio  $\beta = M_2/M_1$  is expected to be close to the cosmological ratio between the dark matter and baryonic densities while in our model  $\beta_{\text{cosm}} = \rho_2/\rho_1 = 10$ . As for the smaller galaxies, they are

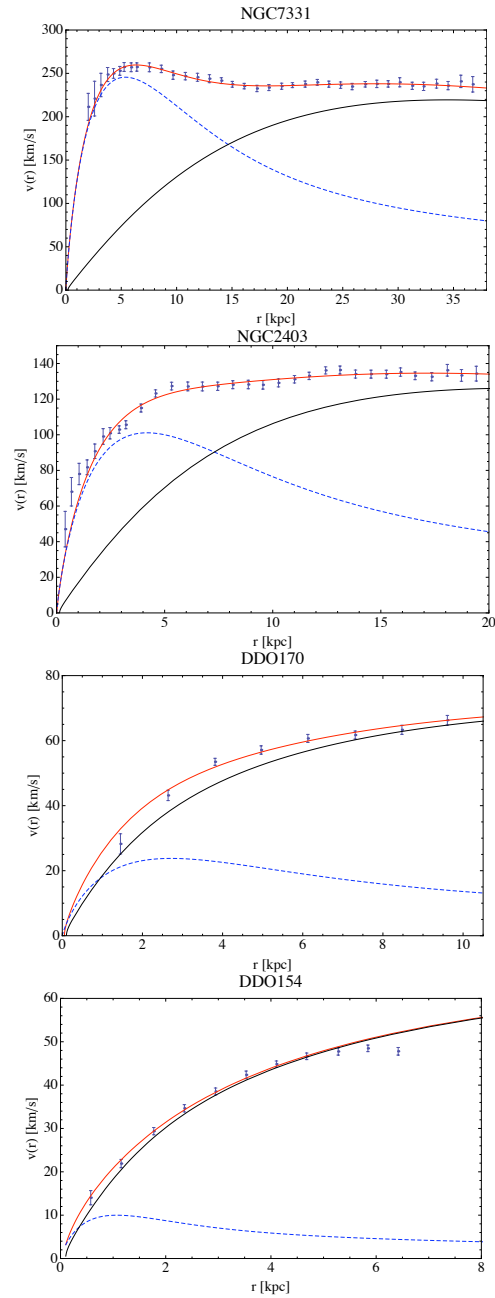


**Fig. 6.** Fit of the rotational curves (solid) for different galaxies using the modified potential and a disc-like distribution for dark matter. In all cases the Yukawa radius is fixed as  $r_m = 10$  kpc. The individual contributions  $v_{\text{dm}}$  from mirror matter and  $v_{\text{vis}}$  from luminous matter (dotted) are also shown. The fit parameters are reported in Table 1.

expected to be more dark matter dominated, with  $\beta > 10$ , as we discuss below. The lower panel of Fig. 5 shows the dependence on the ratio  $\nu = r_m/r_1$ , for a characteristic value  $\beta = 10$ . In both Figs. 5 we assumed that the visible and dark disc density profiles are ‘zoomed’ as  $\alpha = \beta^{1/3}$ . Let us to stress that when gravity is not modified, it is impossible to reproduce the observed rotational curves with both dark and visible discs having the similar density pro-

	NGC7331	NGC2403	DDO170	DDO154
$r_1$	4.5 kpc	2.0 kpc	1.1 kpc	0.50 kpc
$M_L$	54 $M_9$	7.9 $M_9$	0.18 $M_9$	0.05 $M_9$
$M_1$	98 $M_9$	12.6 $M_9$	0.4 $M_9$	0.03 $M_9$
$\gamma = M_1/M_L$	1.8	1.6	2.2	0.6
$M_2$	103 $M_{10}$	26 $M_{10}$	7.6 $M_{10}$	6.0 $M_{10}$
$\beta = M_2/M_1$	10.5	20.6	190	2000
$r_2$	9.0 kpc	3.2 kpc	0.87 kpc	0.66 kpc
$\alpha = r_2/r_1$	2.0	1.6	0.8	1.3
$\chi^2_{\text{d.o.f.}}$	0.8	1.3	1.5	0.6

**Table 1.** The fitting results for different galaxies. Their optical disc length scales  $r_1$  and the “luminosity” related masses  $M_L = (L/L_\odot) M_\odot$  are taken from [2], in units defined as  $M_9 = 10^9 M_\odot$ , etc.;  $M_1, M_2$  and  $r_2$  are the best fit parameters (the contribution of gas is included in  $M_1$ ). For NGC7331 also the bulge contribution was taken into account as in ref. [2].

files (16): the Keplerian tail is always there – see the dotted curves in Fig. 5.

Using the modified potential (6) and assuming a disc-like density profiles for both dark and luminous matter, the rotational curves of different (standard, intermediate and dwarf) galaxies can be well reproduced. As an example, we fit the rotational curves of a number of representative disk galaxies (see Figs. 6). Among the four parameters,  $M_1$ ,  $r_1$  and  $M_2$ ,  $r_2$ , the last two regard the dark matter distribution and are taken as free parameters for fitting the rotational curve of each galaxy. The value of the visible disc length  $r_1$  for each galaxy can be deduced by astrophysical measurements, by extrapolating the optical shape of the galaxy via exponential profile. In other words, the radial distribution of baryonic mass is assumed to be given by the mean radial distribution of light; which is to say, the mass-to-light ratio  $\gamma = M_1/M_L$  is taken to be constant for each particular galaxy, where the value of the luminous mass  $M_L$  is inferred from a total luminosity of the galaxy by taking the average mass-to-luminosity ratio for its stellar population equal to that of the sun. Therefore, the factor  $\gamma$  that takes into account the possible variation of the mass-to-light ratio between different galaxies is taken as a fit parameter, as in ref. [2]. It is natural to expect that for realistic fits its value should not strongly deviate from 1.

In particular, we fit the data relative to a large (NGC 7331) and an intermediate (NGC 2403) mass spiral galaxies, as well as for two dwarfs (DDO154 and DDO170) which presumably are dark matter dominated. The length scales of these galaxies are inferred from their luminosity shape [2]. We find that all the above galaxies can be nicely fitted by the three parameters  $\alpha = r_2/r_1$ ,  $\beta = M_2/M_1$  and  $\gamma = M_1/M_L$ , with  $\chi^2_{\text{dof}} \simeq 1$ . (Let us remark that for the standard dark matter halos with the IT or NFW profiles also 3-parameter fit is needed, with  $\rho_s, r_s$  and  $\gamma = M_1/M_L$  being the relevant parameters.) The gravitational radius is *a priori* fixed to  $r_m = 10$  kpc.<sup>7</sup>

<sup>7</sup> This choice is essentially based on our intuitive guess. For a complete study, a large sample of different galaxies should be analyzed by taking  $r_m$  as a free parameter that is *unique* for all galaxies. Such an analysis may suggest that the best fit value

The fit details are shown in Fig. 6 and Table 1. We see that the smaller galaxies are more dominated by dark matter, which can have an intriguing link with the empiric Tully-Fisher relations. Namely, for a large galaxy with  $M_1 \sim 10^{11} M_\odot$  we have  $\beta \sim 10$ , but for a galaxy with  $M_1 \sim 10^7 M_\odot$  we get  $\beta \sim 10^3$ . This seems quite natural in the context of our model with the Yukawa length  $r_m \sim 10$  kpc. At the scales smaller than  $r_m$  the dark and ordinary components become reciprocally “blind” and so the smaller is the dark matter clump, less it should be capable to capture and hold gravitationally the ordinary baryons. This feature can be translated to the following paradigm: big galaxies are expected have the ratio  $\beta = M_2/M_1$  nearly approaching the cosmological proportion between dark and visible matter as in cosmology:  $\beta_{\text{cosm}} = \rho_2/\rho_1 \simeq 10$  in our case. As for small galaxies, the value of  $\beta$  can be substantially larger: the smaller is the dark matter disc, the less amount of the ordinary baryons it can capture and hold against the galaxy scattering and merging processes and thus should be more dark matter dominated.

For scales  $r > r_m$  gravity is essentially Newtonian, with a constant  $G_N/2$ . Therefore, for normal galaxies one can expect the evidence of quasi-Keplerian fall-off at the distances  $r > 5r_m$ . In principle, such a feature may be traced in large galaxies where the velocities can be measured beyond 50 kpc or so.

Certainly, our scenario of gravity modification can be applied also when dark matter is cold and collisionless (CDM-like) and forms extended halos instead of the discs. In this case, for fitting the rotational curves, the gravitational radius presumably will be somewhat less than 10 kpc, and the rotational curves can be reproduced in the Newton-like large distance limit of the potential (6) with a constant  $G_N/2$ . Therefore, the value of  $\beta = M_2/M_1$  is required to be twice bigger than in the canonical CDM interacting with Newton constant  $G_N$ . The gravity screening between ordinary and dark components at distances  $r < r_m$  would help to avoid the cusp problem: even if the dark matter density distribution has a central singularity, it would not affect the rotational curves at small distances.

for  $r_m$  is different from 10 kpc. However, we do not expect the difference more than a factor 1.5 or so, i.e.  $r_m = 6 \div 15$  kpc.



Notice that, taking  $r_m \sim 10$  kpc, for the galaxy clusters we recover the standard picture if the dark-to-baryon mass ratio in the cluster is  $\beta = 10$  or so. Indeed, the relevant length scales in a cluster are bigger than  $r_m$  and the potential (6) reduces to the Newtonian potential but with a half-strength  $G_N/2$ . Therefore, the velocity dispersions observed in clusters require  $M_2 \simeq 10M_1$ , instead of  $M_2 \simeq 5M_1$  which works when the Newton constant is  $G_N$ .

## 4 Discussion and outlook

Mirror matter is a dark matter candidate that can have interesting applications for many cosmological problems [15,16]. However, being collisional and dissipative, it has difficulties with the formation of extended halos, and thus with the explanation of the galactic rotational velocities. Typically, for fitting the rotational curves without modifying the Newton potential, dark matter profile with a constant inner core is required, as e.g. in refs. [2,3].

In this paper we have shown that the flat rotational curves can be nicely explained by the bi-metric modification of gravity suggested in ref. [28] where the hidden mirror sector is equipped by its own mirror gravity. In other words, if the Universe is made of two separate gauge sectors, one visible and the other mirror, each of them can have its own gravity. The two metrics can interact leading to a large distance Yukawa-type modification of the gravitational force. At small distances, where the gravitational interaction between the different sectors is effectively shut off, the behavior is practically Newtonian.

Though the structure formation process is very complicated, some simple conclusions can be drawn. Dark matter is more abundant and it will start collapsing before the ordinary matter forming gravitational wells for capturing the latter. In difference from the CDM, the collisional MDM is tended to undergo a dissipative collapse creating structures as galaxies, similar to the visible ones, with similar mass distribution. Hence, it is natural to expect that similarly to the visible matter, mirror matter forms galactic discs. Since the gravitational force between sectors 1 and 2 is effective at distances  $r \gtrsim r_m \sim 10$  kpc, after an initial stage of mutual interaction, as the collapse proceeds, the inner structures of dark and ordinary matter are formed with a weaker correlation. On the contrary, one can argue that for the outer region of galaxies, the interaction between ordinary and dark matter is important for angular momentum exchange giving rise to a common galactic plane.

It is important, that a good dark matter candidate together with a plausible gravity modification should reproduce the observed rotational curves for the galaxies of different size and type. We have shown that the rotational curves can be explained if the dark and visible matter components both have similar mass distributions in discs, with exponential density profiles  $\sigma_{1,2}(r) \propto e^{-r/r_{1,2}}$ , where  $r_1, r_2$  respectively are the length scales of the visible and dark discs. Let us remark, however, that our proposal of gravity modification would work even if dark matter behaves as the CDM, avoiding the tension between the observed

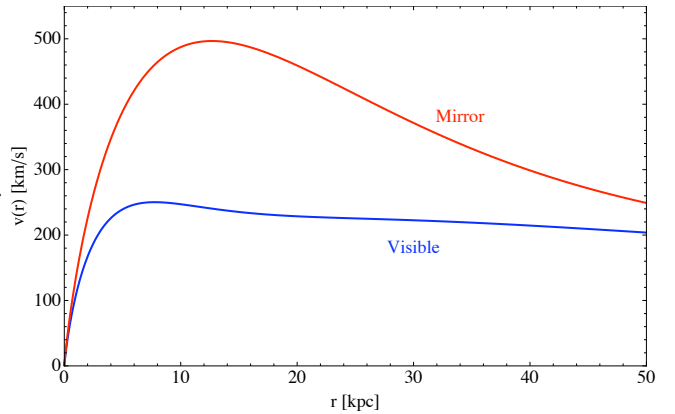


**Fig. 7.** Velocity curves for ordinary and mirror particles in a typical galaxy similar to the Milky Way, with  $M_1 = 5 \times 10^{11} M_\odot$  and  $r_1 = 3$  kpc. For a dark disc, we take  $M_2 = 5 \times 10^{12} M_\odot$  and  $r_2 = 7$  kpc. The enhancement of the dark matter velocity is important for its direct detection.

rotational curves and the cusped halos predicted by N-body numerical simulations. The idea is that dark matter does not gravitate with normal matter at small distances and the dark matter cusp would not affect the shape of velocity curves.

Observations also show that in a galaxy the dark-to-visible matter ratio fractions sharply increases with decreasing luminosity (see Table 1). This property is natural in our model, where the graviton Compton length  $r_m$  is of order 10 kpc and at smaller scales the dark and ordinary components become rather “blind” to each other. Therefore, the smaller is the dark matter disc, the less amount of the ordinary baryons it can capture and thus should be more dark matter dominated. For scales  $r \gg r_m$  gravity is essentially Newtonian and in very large galaxies with an optical radius greater than 50 kpc or so the rotational curves should show the quasi-Keplerian fall-off. This can be interpreted in standard paradigm as a fact that the bigger galaxies have less fraction of dark matter, approaching the cosmological proportion between  $\rho_D$  and  $\rho_B$  (about 10 in our case), while the small galaxies should be more dominated by dark matter.

The following remark is in order. As far as the galaxies and clusters are regarded, the “Newtonian” character of our gravity at large distances, with  $G(r > r_m) = G_N/2$  but  $\beta \sim 10$ , will have the similar effect as the extended dark matter halos also concerning the gravitational lensing as far as it essentially imitates the similar shape of the gravitational potential. As for the microlensing events by Machos and other compact objects in the Milky Way and its neighborhoods, were the relevant distances are of the order of the stellar size at which the dark matter remains gravitationally “invisible”, the corresponding dynamics should be governed exclusively by the standard gravity with the canonical Newton constant  $G_N$ .

Intriguingly, recent astrophysical observations indicate a peculiar behavior of dark matter in galaxy cluster collisions. In the Bullet cluster [39], the dark matter component of the cluster shows a collisionless behavior. Instead,

in the Abell 520 cluster [40] there is an evidence for an important contribution from self-interaction. In mirror dark matter models those observations are not surprising [41].

At large cosmological distance both sectors are mutually interacting with an effective Newton constant  $G_N/2$ . One can argue then that the observed Hubble constant requires that the total energy density of the Universe is twice bigger than in the standard cosmology in which the Newton constant at cosmological distances remains the canonical  $G_N$ . In this scenario, instead of  $\rho \approx \rho_{cr} = 3H_0^2/8\pi G_N$  of the standard FRW cosmology, we expect  $\rho_{our} \approx 2\rho_{cr} = 3H_0^2/4\pi G_N$ .

The mirror matter model with modified potential does not exclude the possibility of a direct (non-gravitational) interaction between normal and dark matter components. For example, the photon - mirror photon kinetic mixing  $\frac{\epsilon}{2}F_1^{\mu\nu}F_{2\mu\nu}$  [17] that effectively renders mirror particles ‘millicharged’ with respect to ordinary electromagnetic interactions. In this way, mirror nuclei can scatter off the ordinary nuclei in the experimental set up for the dark matter direct detection and thus leave their trace on the recoil energy spectrum of the latter. This process might be suitable for explaining the results of the DAMA/Libra experiment [42], if  $\epsilon \sim 10^{-9}$  and the mirror sector is dominated by the oxygen or other mirror elements with comparable mass [43]. However, such a large value of  $\epsilon$  seems to be in tension with the cosmological limits on the mirror particle electric charges [44] while the large oxygen fraction is also questionable.

It is worth to point out that in our model the observed shape of the velocities requires at least twice the amount of dark matter in our galaxy than the CDM scenario. In addition, if it is distributed in a disc, then the local density of dark matter should be much larger than in the case of extended quasi-spherical halos. On the other hand, gravity is not universal in our model, and thus ordinary and mirror objects in the galaxy should have different accelerations. Namely, the typical velocities of dark matter particles in the Milky Way at the distances of 10 kpc in our scenario approach 500 km/s, while the velocities of the ordinary matter (and sun itself) are around 200 km/s (see Fig. 7). Both of these features are of interest for dark matter searches, since they enhance the chance of a direct detection in experiments like DAMA [42]. Namely, if the MDM has a local density much larger than the one inferred from the CDM halo profile, this would make the smaller values  $\epsilon \ll 10^{-9}$  effective for dark matter detection. On the other hand, if the typical velocities of dark matter particles are more than twice larger than what is assumed in the case of CDM halos, then for producing a signal with a recoil energies in the range 2-6 keV, the ‘‘bigravitating’’ dark matter particles may be lighter than normally gravitating dark matter particles for which the typical velocities around 200-300 km/s are inferred. In particular, instead of mirror oxygen, the element that becomes operative is mirror helium, which is expected to be a dominant component in mirror sector [23].

Our scenario can have also rather interesting implications for neutrino-mirror neutrino (active-sterile) oscilla-

tions [18], making more attractive the case of an exact mirror parity where the ordinary and mirror neutrinos are degenerate in mass and maximally mixed. Their oscillations inside the galaxy should suffer an MSW-like suppression because of different gravitational potentials felt by active and sterile neutrino species. Far outside the galaxy where the gravity becomes universal oscillations instead can proceed in full strength.

## Acknowledgments

We thank F. Nesti and P. Salucci for useful discussions and comments. This work is partially supported by the European FP6 Network ‘‘UniverseNet’’ MRTN-CT-2006-035863 and in part by the MIUR biennial grant for the Research Projects of the National Interest PRIN 08 on ‘‘Astroparticle Physics’’.

## References

1. J. N. Bahcall and R. M. Soneira, *Astrophys. J. Suppl.* **44** (1980) 73.
2. K. G. Begeman, A. H. Broeils and R. H. Sanders, *Mon. Not. Roy. Astron. Soc.* **249** (1991) 523.
3. A. Burkert, *Astrophys. J.* **447** (1995) L25.
4. J. F. Navarro, C. S. Frenk and S. D. M. White, *Mon. Not. Roy. Astron. Soc.* **275** (1995) 720; *Astrophys. J.* **490** (1997) 493.
5. B. Moore et al., *Mon. Not. Roy. Astron. Soc.* **310** (1999) 1147; *Phys. Rev. D* **64** (2001) 063508.
6. P. Salucci et al., *Mon. Not. Roy. Astron. Soc.* **378** (2007) 41 [arXiv:astro-ph/0703115].
7. P. Salucci, F. Walter and A. Borriello, *A&A* **409** (2003) 53; G. Gentile et al., *Astrophys. J.* **634** (2005) 145.
8. K. Spekkens and R. Giovanelli, arXiv:astro-ph/0502166.
9. P. Salucci et al., *Mon. Not. Roy. Astron. Soc.* **378** (2007) 41.
10. I. Yu. Kobzarev, L. B. Okun and I. Ya. Pomeranchuk, *Sov. J. Nucl. Phys.* **3** (1966) 837.
11. S. G. Blinnikov and M. Yu. Khlopov, *Sov. Astron.* **27** (1983) 371.
12. R. Foot, H. Lew and R. R. Volkas, *Phys. Lett. B* **272** (1991) 67.
13. T. D. Lee and C. N. Yang, *Phys. Rev.* **104** (1956) 254.
14. K. Nishijima and M. H. Saffouri, *Phys. Rev. Lett.* **14** (1964) 205.
15. Z. Berezhiani, *Int. J. Mod. Phys. A* **19** (2004) 3775, arXiv:hep-ph/0312335; ‘‘Through the Looking-Glass: Alice’s Adventures in Mirror World,’’ in *Ian Kogan Memorial Collection ‘‘From Fields to Strings: Circumnavigating Theoretical Physics’’*, ed. by M. Shifman et al. (World Scientific, Singapore, 2005), vol. 3, pp. 2147-2195, arXiv:hep-ph/0508233.
16. Z. Berezhiani, *Eur. Phys. J. ST* **163** (2008) 271; *AIP Conf. Proc.* **878** (2006) 195, arXiv:hep-ph/0612371.
17. B. Holdom, *Phys. Lett. B* **166** (1986) 196; S. L. Glashow, *Phys. Lett. B* **167** (1986) 35; E. D. Carlson and S. L. Glashow, *Phys. Lett. B* **193** (1987) 168.

18. R. Foot, H. Lew and R. R. Volkas, *Mod. Phys. Lett. A* **7** (1992) 2567;  
E. K. Akhmedov, Z. Berezhiani and G. Senjanović, *Phys. Rev. Lett.* **69** (1992) 3013;  
R. Foot and R. R. Volkas, *Phys. Rev. D* **52** (1995) 6595;  
Z. Berezhiani and R. N. Mohapatra, *Phys. Rev. D* **52** (1995) 6607.
19. Z. Berezhiani and L. Bento, *Phys. Rev. Lett.* **96** (2006) 081801 [arXiv:hep-ph/0507031]; *Phys. Lett. B* **635** (2006) 253 [arXiv:hep-ph/0602227].
20. Z. Berezhiani, *Eur. Phys. J. C* **64** (2009) 421 [arXiv:0804.2088 [hep-ph]].
21. Z. Berezhiani, *Phys. Lett. B* **417** (1998) 287.
22. Z. Berezhiani, A. D. Dolgov and R. N. Mohapatra, *Phys. Lett. B* **375** (1996) 26; *Acta Phys. Polon.* **B 27** (1996) 1503.
23. Z. Berezhiani, D. Comelli and F. L. Villante, *Phys. Lett. B* **503** (2001) 362.
24. A. Ignatiev and R. R. Volkas, *Phys. Rev. D* **68** (2003) 023518.
25. Z. Berezhiani, P. Ciarcellutti, D. Comelli, F. L. Villante, *Int. J. Mod. Phys. D* **14** (2005) 107.
26. Z. Berezhiani, S. Cassisi, P. Ciarcelluti and A. Pietrinferni, *Astropart. Phys.* **24** (2006) 495.
27. L. Bento and Z. Berezhiani, *Phys. Rev. Lett.* **87** (2001) 231304; *Fortsch. Phys.* **50** (2002) 489; arXiv:hep-ph/0111116
28. Z. Berezhiani, F. Nesti, L. Pilo and N. Rossi, *JHEP* **0907** (2009) 083, arXiv:0902.0144 [hep-th].
29. Z. Berezhiani, D. Comelli, F. Nesti and L. Pilo, *Phys. Rev. Lett.* **99** (2007) 131101, arXiv:hep-th/0703264.
30. Z. Berezhiani and O. V. Kancheli, arXiv:0808.3181 [hep-th].
31. C. J. Isham, A. Salam and J. A. Strathdee, *Phys. Rev. F* **3** (1971) 867.
32. T. Damour and I. I. Kogan, *Phys. Rev. D* **66** (2002) 104024 [arXiv:hep-th/0206042].
33. N. Boulanger, T. Damour, L. Gualtieri and M. Henneaux, *Nucl. Phys. B* **597**, (2001) 127 [arXiv:hep-th/0007220].
34. V. A. Rubakov, arXiv:hep-th/0407104.
35. Z. Berezhiani, D. Comelli, F. Nesti and L. Pilo, *JHEP* **0807** (2008) 130, arXiv:0803.1687 [hep-th]
36. T. Clifton, M. Banados and C. Skordis, arXiv:1006.5619 [gr-qc].
37. N. Rossi, *Eur. Phys. J. ST* **163** (2008) 291.
38. K. C. Freeman, *Astrophys. J.* **160**, 811 (1970).
39. M. Jee *et al.*, *Astrophys. J.* **618**, 46 (2004), arXiv:astro-ph/0409304.
40. A. Mahdavi, H. Hoekstra, A. Babul, D. D. Balam and P. L. Capak, arXiv:0706.3048 [astro-ph].
41. Z. K. Silagadze, *ICFAI U. J. Phys.* **2** (2009) 143 [arXiv:0808.2595 [astro-ph]].
42. R. Bernabei *et al.* [DAMA Collaboration], *Eur. Phys. J. C* **56**, 333 (2008), arXiv:0804.2741 [astro-ph].
43. R. Foot, *Phys. Rev. D* **78**, 043529 (2008), arXiv:0804.4518 [hep-ph]
44. Z. Berezhiani and A. Lepidi, *Phys. Lett. B* **681** (2009) 276 [arXiv:0810.1317 [hep-ph]].